J|A|C|S
COMMUNICATIONS

BaGe$_5$: A New Type of Intermetallic Clathrate

Umut Aydemir, Lev Akselrud, Wilder Carrillo-Cabrera, Christophe Candolfi, Niels Oeschler,
Michael Baitinger, Frank Steglich, and Yuri Grin*

Max-Planck-Institut für Chemische Physik fester Stoffe, Dresden 01187, Germany

Received May 15, 2010; E-mail: grin@cpfs.mpg.de

Abstract: BaGe$_5$ constitutes a new type of intermetallic clathrate obtained by decomposition of clathrate-I Ba$_8$Ge$_{43}\square_3$ at low temperatures. The crystal structure consists of characteristic layers interconnected by covalent bonds. BaGe$_5$ is a semiconducting Zintl phase.

Intermetallic clathrates constitute a class of cage compounds in which electropositive metal atoms are encapsulated in covalent frameworks of mainly Group 14 elements (Si, Ge, Sn). The crystal structures commonly found are related to the type I and type II gas hydrates.[1] By increasing the content of electropositive elements, related crystal structures form which have no corresponding gas hydrate structure, e.g., the clathrate type *cP*124.[2] In the binary system Ba−Ge, two clathrate types have been reported, namely the clathrate *cP*124 Ba$_6$Ge$_{25}$[3] and the clathrate-I Ba$_8$Ge$_{43}\square_3$ ($\square$ stands for vacancy).[4] Here we report on the synthesis, crystal structure, and physical properties of BaGe$_5$, which constitutes a new clathrate type, *oP*60, with the orthorhombic space group *Pmna* (Figure 1a). The compound is a diamagnetic semiconducting Zintl phase and represents a new prototype structure for thermoelectric materials.[5]

BaGe$_5$ was originally detected by optical and scanning electron microscopy within grains of Ba$_8$Ge$_{43}\square_3$.[4a] However, according to the binary phase diagram,[4a] the two phases are not in thermal equilibrium. Ba$_8$Ge$_{43}\square_3$ forms as a high-temperature phase at 770 °C from Ba$_6$Ge$_{25}$ and α-Ge and decomposes peritectically at 810 °C to α-Ge and the respective melt. All attempts to react Ba$_6$Ge$_{25}$ with α-Ge to BaGe$_5$ at temperatures below 770 °C failed. Quenching of a melt with nominal composition BaGe$_5$ between steel plates[4c] results in Ba$_6$Ge$_{25}$ along with Ba$_8$Ge$_{43}\square_3$. By slow cooling over several hours to room temperature, a mixture of Ba$_6$Ge$_{25}$ and α-Ge is obtained. After solidifying the melt within 2−3 min, BaGe$_5$ could be identified along with Ba$_8$Ge$_{43}\square_3$, Ba$_6$Ge$_{25}$, and α-Ge. Obviously, BaGe$_5$ forms via decomposition of Ba$_8$Ge$_{43}\square_3$ but only at low temperatures:

$$\mathrm{Ba_8Ge_{43}\square_3 \rightarrow 8BaGe_5 + 3Ge} \tag{1}$$

The preparation of phase-pure Ba$_8$Ge$_{43}\square_3$ was recently achieved by rapid quenching,[4c] thus allowing for detailed investigations of its decomposition along with the formation of BaGe$_5$. Bulk pieces of Ba$_8$Ge$_{43}\square_3$ were annealed in glassy carbon crucibles under Ar atmosphere at various temperatures between 300 °C and 790 °C. Annealing at 300 °C for 40 d resulted in the complete disproportionation of Ba$_8$Ge$_{43}\square_3$ into a microcrystalline product of BaGe$_5$ and α-Ge (∼5 wt %). At 400 °C, the conversion of Ba$_8$Ge$_{43}\square_3$ was complete within 12 h (Supporting Information (SI), Figure S1); at 520 °C it was complete within 1 h. No decomposition of BaGe$_5$ was detected after further annealing for 7 weeks at 520 °C. Differential scanning calorimetry of BaGe$_5$ on heating (SI, Figure S2, p S9) showed a broad endothermic signal at ∼590 °C, indicating the peritectoid transformation into Ba$_6$Ge$_{25}$ and α-Ge. From long-time annealing experiments on BaGe$_5$, the peritectoid temperature was estimated to be ∼550 °C. Hence, contrary to the previous conclusion,[4a] BaGe$_5$ is an equilibrium phase. A direct reaction of BaGe$_2$ or Ba$_6$Ge$_{25}$ with α-Ge, which should yield BaGe$_5$, was found to be kinetically hindered below 550 °C. The

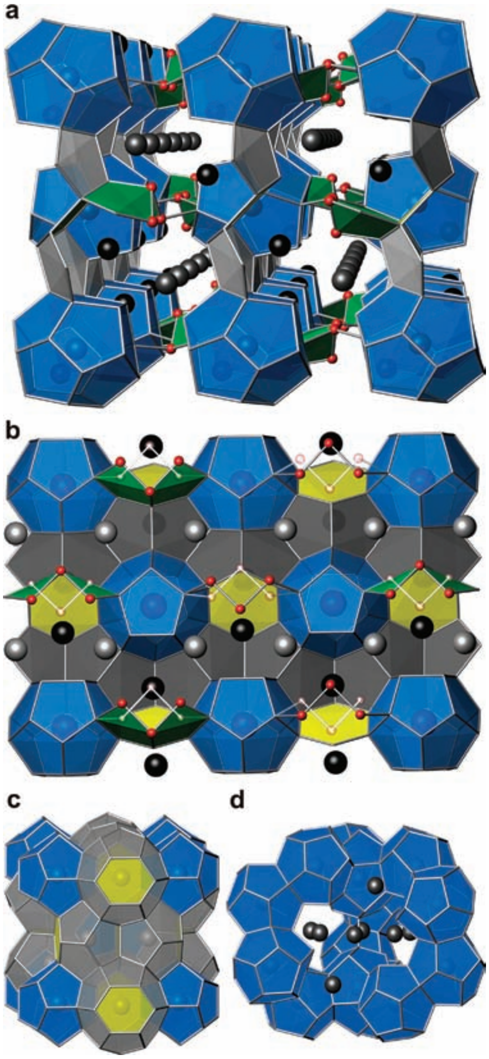

Figure 1. (a) Crystal structure of BaGe$_5$ with channels and covalently bonded layers along [100]. (b) Perpendicular view down [010]. Ba1 inside blue dodecahedra, Ba2 in gray, Ba3 in black, alternatively occupied Ge sites in red and white. Respective features in clathrate-I (c) and clathrate *cP*124 (d).

10.1021/ja104197c

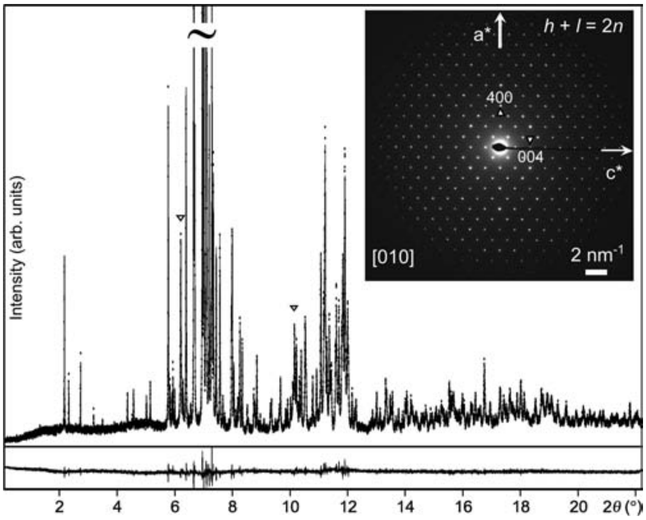

Figure 2. Synchrotron powder X-ray diffraction pattern of $BaGe_5$ ($\lambda = 0.35415$ Å, dotted line) with the calculated profile after Rietveld refinement (solid line) and difference curve (below). The two most intense α-Ge reflections are marked. Inset: Selected area electron diffraction pattern along [010] in TEM.

conversion of $Ba_8Ge_{43}\square_3$ to $BaGe_5$ and α-Ge is reversible. Phase-pure $Ba_8Ge_{43}\square_3$ was retrieved after annealing $BaGe_5$ and α-Ge at 790 °C for 2 weeks.

Synchrotron powder diffraction data were collected for $BaGe_5$ obtained at 400 °C (Figure 2; SI, p. S7). Besides the reflections of α-Ge, all reflections were indexed on the basis of a primitive orthorhombic unit cell.[6] Structure solution succeeded in space group *Pmna* by use of powder X-ray and electron diffraction data (SI, pp S7−S8). Rietveld refinement[7] revealed the chemical composition $BaGe_5$, in good agreement with results from wavelength-dispersive X-ray spectroscopy ($Ba_{0.98(1)}Ge_{5.02(1)}$, SI, p S9). The crystal structure of $BaGe_5$ may be described as intermediate between $Ba_8Ge_{43}\square_3$ (clathrate-I, Figure 1c) and Ba_6Ge_{25} (clathrate *cP*124, Figure 1d). It contains only one type of polyhedral cages, Ge_{20} dodecahedra centered by Ba1 atoms, arranged on a B-centered orthorhombic lattice. Ba2 atoms are assembled in channels, in analogy to Ba_6Ge_{25}, while Ba3 atoms are located in cavities resembling the Ge_{24} polyhedra of $Ba_8Ge_{43}\square_3$. The Ge_{20} dodecahedra in $BaGe_5$ are connected via pentagons and hexagons to 2D layers perpendicular to [010]. Similar layers, but fully separated from each other, have been observed in the crystal structure of $A_3Na_{10}Sn_{23}$ (A = Cs, Rb, K).[8] In $BaGe_5$, the layers are interconnected by covalent bonds via $(3b)Ge^-$ species. These atoms occupy alternatively two crystallographic sites with occupancy of 0.5, introducing disorder in the crystal structure. An ordered arrangement of $(3b)Ge^-$ atoms in isomorphic subgroups of *Pmna* could not be revealed from Rietveld refinements.

Twenty Ge atoms per unit cell ($Z = 10$) are three-bonded, leading to the electronic balance $[Ba^{2+}]_{10}[(3b)Ge^-]_{20}[(4b)Ge^0]_{30}$. Hence, $BaGe_5$ can be considered a Zintl phase, which is further corroborated by measurements of the physical properties (SI, p. S10). In contrast, the clathrates Ba_6Ge_{25} and $Ba_8Ge_{43}\square_3$ contain excess electrons according to $[Ba^{2+}]_6[(3b)Ge^-]_8\ [(4b)Ge^0]_{17} \times 4e^-$ and $[Ba^{2+}]_8[(3b)Ge^-]_{12}[(4b)Ge^0]_{31} \times 4e^-$, respectively, and are metals. $BaGe_5$ is diamagnetic in the whole investigated temperature range, with $\chi \approx -210 \times 10^{-6}$ emu mol^{-1} at 300 K (Figure 3a). A rough estimate of the diamagnetic contribution using the tabulated diamagnetic increments for Ba^{2+} cations[9a] and for Ge atoms in α-Ge[9b] gives $\chi_{calc} \approx -110.5 \times 10^{-6}$ emu mol^{-1}. The lower experimental value might be due to the contribution of the Ge^- anions, for which no increments have been reported yet. The temperature dependence of the electrical resistivity indicates a semiconducting behavior (Figure 3b). The small hump observed around 170 K might point to the ordering of the $(3b)Ge^-$ atoms, similar to what was observed for Ba_6Ge_{25}.[3c] To understand the anomalous conduction behavior, further investigations are required.

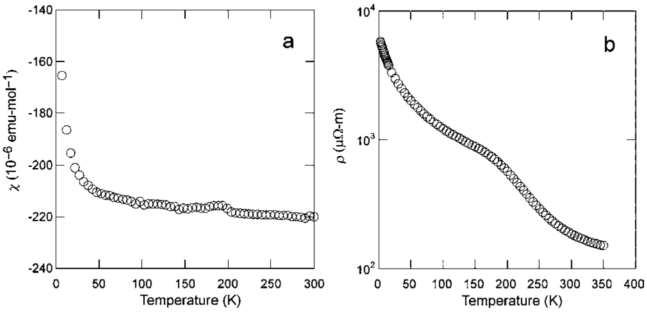

Figure 3. (a) Magnetic susceptibility $\chi(T)$ and (b) electrical resistivity ρ(T) of $BaGe_5$ at low temperatures.

$BaGe_5$ is a Zintl phase crystallizing with a new clathrate type. The compound was obtained from decomposition of $Ba_8Ge_{43}\square_3$ at different temperatures between 300 °C and 520 °C. Its semiconducting behavior together with a complex crystal structure may lead to interesting thermoelectric properties.

Acknowledgment. We thank I. Margiolaki and Yu. Prots for the synchrotron X-ray measurements at ESRF in Grenoble, P. Marasas and S. Hoffmann for thermal analysis, and the competence groups *Struktur* and *Metallographie* at MPI CPfS for technical assistance. H. Borrmann is acknowledged for valuable discussions. C.C. and M.B. acknowledge financial support from the CNRS-MPG program and the DFG priority program SPP1415, respectively.

Supporting Information Available: Experimental details and crystallographic data (PDF, CIF). This material is available free of charge via the Internet at http://pubs.acs.org.

References

(1) Jeffrey, G. A. In *Inclusion Compounds I*; Atwood, J. L., Davies, J. E. D., MacNicol, D. D., Eds.; Academic Press: London, 1984; pp 135−190.

(2) Von Schnering, H. G.; Zürn, A.; Chang, J.-H.; Baitinger, M.; Grin, Yu. *Z. Anorg. Allg. Chem.* **2007**, *633*, 1147.

(3) (a) Carrillo-Cabrera, W.; Curda, J.; von Schnering, H. G.; Paschen, S.; Grin, Yu, *Z. Kristallogr.* **2000**, *215*, 207. (b) Fukuoka, H.; Iwai, K.; Yamanaka, S.; Abe, H.; Yoza, K.; Häming, L. *J. Solid State Chem.* **2000**, *151*, 117. (c) Carrillo-Cabrera, W.; Borrmann, H.; Paschen, S.; Baenitz, M.; Steglich, F.; Grin, Yu. *J. Solid State Chem.* **2005**, *178*, 715.

(4) (a) Carrillo-Cabrera, W.; Budnyk, S.; Prots, Y.; Grin, Yu. *Z. Anorg. Allg. Chem.* **2004**, *630*, 2267. (b) Okamoto, N. L.; Tanaka, K.; Inui, H. *Acta Mater.* **2006**, *54*, 173. (c) Aydemir, U.; Candolfi, C.; Borrmann, H.; Baitinger, M.; Ormeci, A.; Carrillo-Cabrera, W.; Chubilleau, C.; Lenoir, B.; Dauscher, A.; Oeschler, N.; Steglich, F.; Grin, Yu. *Dalton Trans.* **2010**, *39*, 1078.

(5) (a) Nolas, G. S.; Slack, G. A.; Schujman, S. B. In *Semiconductors and Semimetals*; Tritt, T. M., Ed.; Academic Press: San Diego, 2000; Vol. 69, p 255. (b) Kleinke, H. *Chem. Mater.* **2010**, *22*, 604.

(6) Crystallographic data of $BaGe_5$: space group *Pmna*, $a = 10.727(1)$ Å, $b = 9.2844(7)$ Å, $c = 14.794(1)$ Å; 2 Ba in 2*a* 000; 4 Ba in 4*g* $^1/_4$ *y* $^1/_4$, $y = 0.4237(3)$; 4 Ba in 4*h* 0*yz*, $y = 0.2047(3)$, $z = 0.6324(2)$; 4 Ge in 4*h* 0*yz*, $y = 0.3640(4)$, $z = 0.1101(3)$; 4 Ge in 4*h* 0*yz*, $y = 0.2136(4)$, $z = 0.3807(3)$; 4 Ge in 4*h* 0*yz*, $y = 0.1450(4)$, $z = 0.2146(3)$; 2 Ge in 4*h* 0*yz*, $y = 0.4667(9)$, $z = 0.4090(5)$; 4 Ge in 8*i* *xyz*, $x = 0.3376(4)$, $y = 0.5072(8)$, $z = 0.0309(3)$; 8 Ge in 8*i* *xyz*, $x = 0.3049(3)$, $y = 0.0939(3)$, $z = 0.0608(2)$; 8 Ge in 8*i* *xyz*, $x = 0.1194(3)$, $y = 0.7215(3)$, $z = 0.1550(2)$; 8 Ge in 8*i* *xyz*, $x = 0.1807(3)$, $y = 0.3083(3)$, $z = 0.0060(2)$; 8 Ge in 8*i* *xyz*, $x = 0.3180(3)$, $y = 0.0205(3)$, $z = 0.6850(2)$; $R_i = 0.066$; $R_p = 0.107$; $R_{wp} = 0.086$; cf. SI, Tables S1 and S2.

(7) Akselrud, L. G.; Zavalii, P. Y.; Grin, Yu.; Pecharsky, V. K.; Baumgartner, B.; Wölfel, E. *Mater. Sci. Forum* **1993**, *335*, 133.

(8) Bobev, S.; Sevov, S. C. *Inorg. Chem.* **2000**, *39*, 5930.

(9) (a) Weiss, A.; Witte, H. *Magnetochemie*; Verlag Chemie, Weinheim/Bergstr., 1973; p 72. (b) Madelung, O.; Rössler, U.; Schulz, M. *Group III Condensed Matter*; Landolt−Börnstein V41A1b; Springer-Verlag: Berlin, 2002.

JA104197C